

Tunable Photoluminescence Properties of Fluorescein in a Layered Double Hydroxide Matrix by Changing the Interlayer Microenvironment

Wenyong Shi, Zhiyong Sun, Min Wei,* David G. Evans, and Xue Duan

State Key Laboratory of Chemical Resource Engineering, Beijing University of Chemical Technology, Beijing 100029, P. R. China

Received: July 26, 2010; Revised Manuscript Received: October 26, 2010

This paper reports a novel method to tune the fluorescence properties of fluorescein (FLU) in a 2D matrix of layered double hydroxide (LDH) by changing the interlayer microenvironment. FLU and surfactants with different alkyl chain lengths were cointercalated in the galleries of a Zn_2Al LDH by the anion exchange method. Thin films of $FLU-C_nH_{2n+1}SO_3/LDH$ ($n = 5, 6, 7, 10,$ and 12 , respectively; n stands for the number of carbon in the alkyl chain), which possess a well c -orientation revealed by XRD and SEM, were obtained by the solvent evaporation method on Si substrates. It was found that the orientation of FLU and its anisotropy, fluorescence wavelength, fluorescence quantum yield, and lifetime correlate with the microenvironment of the LDH gallery, which can be tuned by simply changing the alkyl chain length of the surfactant. The optimal fluorescence quantum yield, anisotropy, the longest fluorescence lifetime and the strongest photostability of the $FLU-C_nH_{2n+1}SO_3/LDH$ film can be obtained with $n = 7$, due to the “size-matching” rule between the organic dye and surfactant.

1. Introduction

The organic tunable lasers generally used in liquid-state active media have been intensively investigated in the past decade. However, the liquid-state dye lasers are limited to a great extent in practical applications, owing to the involvement of a large circulator with toxic solvents, careful maintenances and extremely poor recycling. The development of solid-state tunable lasers with interesting technological innovations such as compactness or miniaturization, could solve these problems. Tunable solid-state lasers can be obtained by the incorporation of laser dyes as guest compounds in host solid materials. Recently, several light-emitting solid systems based on the inclusion of laser dyes into solid matrices have been reported.¹

Among the inorganic matrices for organic dye molecules, the 2-dimensional layered double hydroxide (LDH) materials have attracted much attention. The LDHs generally expressed as $[M^{II}_xM^{III}_y(OH)_2(A^{n-})_{x/n} \cdot mH_2O]$ (where M^{II} and M^{III} are divalent and trivalent metals, respectively, and A^{n-} an n -valent anion), represent a large versatility in terms of their ability for constructing 2D-organized intercalated compounds.² According to the specific structure of LDHs, new systems based on the intercalation of xanthene dyes in LDHs have been recently reported by Costantino et al.³ and our group.⁴ It has been confirmed that the incorporation of dyes in the LDH gallery improves the photophysical properties of dyes compared with those of their solutions. However, aggregation of fluorescence dyes still can be found in some dye–LDH systems, resulting in a decrease in the fluorescence capability and the photonic facilities.⁵ Therefore, much effort was focused on the inhibition of dye aggregation, for instance, by modification of the physicochemical characteristics of the interlayer region of clays.⁶

Taking into account that the aggregation of dyes in liquid solutions is drastically reduced in hydrophobic media,⁷ the cointercalation of a xanthene dye and a hydrophobic dispersant

(generally surfactant) in the LDH gallery could be an effective strategy for preventing the aggregation of dye. First, surfactant provides a fluorophore with a homogeneous and nonpolar environment and thus reduces the fluorescence quenching by preventing nonradiative processes. Second, the coexisting surfactant may show influences on the orientation and aggregation type of the intercalated dye molecules, reducing intermolecular quenching and improving fluorescence efficiency. Therefore, the study on effects of surfactant on the microenvironment of the LDH gallery is essential for obtaining dye–LDH composites with high luminescence efficiency.

In our previous work,⁸ the cointercalation of α -naphthalene acetate (α -NAA) and 1-heptanesulfonic acid sodium (HES) in the galleries of a Zn_2Al LDH was performed, and the photoluminescence properties of the inorganic–organic composite were finely controlled by varying the fluorophore content through changing the molar ratio of fluorophore/HES. In this study, we further investigated the effect of surfactant polarity on photoluminescence properties of fluorescein (FLU) intercalated in the LDH gallery. FLU (Figure S1–F, Supporting Information), a xanthene dye, was first developed in the 19th century.⁹ FLU and its derivatives have been commonly used as fluorescence indicators and tags, pH probes of intercellular fluids, fluorescence probes, and fluorescence sensors for biogenic matter,¹⁰ due to their large extinction coefficients, high quantum yields, and biological tolerance. The $FLU-C_nH_{2n+1}SO_3/LDH$ ($n = 5, 6, 7, 10,$ and 12 ; n stands for the number of carbons in the alkyl chain of the surfactant; see Figure S1, Supporting Information) composites with the same molar ratio of FLU/surfactant were prepared by the ion-exchange method, and then their thin films on Si substrates were obtained by the solvent evaporation method. It was found that the orientation of FLU and its anisotropic value, fluorescence wavelength, fluorescence quantum yield and lifetime correlate with the microenvironment of the LDH gallery and can be controlled by simply changing the alkyl chain length of surfactant. The optimal fluorescence quantum yield, anisotropy, the longest fluorescence lifetime, and

* Corresponding author. Phone: +86-10-64412131. Fax: +86-10-64425385. E-mail: weimin@mail.buct.edu.cn.

photostability of FLU- $C_nH_{2n+1}SO_3/LDH$ can be obtained with $n = 7$, due to the “size-matching” rule between the organic dye and surfactant. Therefore, this work not only gives a detailed understanding for the influences of microenvironment on the photoluminescence properties of interlayer FLU but also provides a new way for the design and preparation of highly active solid-state dye laser.

2. Experimental Section

2.1. Materials. Sodium FLU and $C_nH_{2n+1}SO_3$ ($n = 5, 6, 7, 10, 12$, respectively) (biochemistry grade) were purchased from Sigma-Aldrich Co. Analytical grade chemicals including $Zn(NO_3)_2 \cdot 6H_2O$, $Al(NO_3)_3 \cdot 9H_2O$, and NaOH were used without further purification. The deionized and decarbonated water was used in all these experimental processes.

2.2. Synthesis of FLU and $C_nH_{2n+1}SO_3$ Cointercalated Zn_2Al LDH. The Zn_2Al-NO_3 LDH precursor was synthesized by the hydrothermal method reported previously.¹¹ Subsequently, the FLU and $C_nH_{2n+1}SO_3$ cointercalated LDH composites were prepared following the ion-exchange method. FLU (5.58×10^{-6} mol) and $C_nH_{2n+1}SO_3$ (5.58×10^{-3} mol) were dissolved in 150 mL of water/ethanol mixture solvent (1:1, v/v), which was then adjusted to pH = 7.0 with a NaOH (0.2 mol/L) solution. A freshly prepared Zn_2Al-NO_3 LDH (0.5 g) was dispersed in the solution thoroughly. The suspension was adjusted to pH = 7.0 and held at room temperature under a N_2 atmosphere for 48 h. The resulting product FLU- $C_nH_{2n+1}SO_3/LDH$ was washed extensively with water.

2.3. Fabrications of the FLU-(CH_2) $_nSO_3/LDH$ Thin Films. Thin films of FLU- $C_nH_{2n+1}SO_3/LDH$ were fabricated by the solvent evaporation method. Substrates of Si wafer were first cleaned by immersing in a bath of deionized water and ethanol in an ultrasonic bath for 30 min. Pasty FLU- $C_nH_{2n+1}SO_3/LDH$ (0.05 g) was suspended in 20 mL of water under a N_2 atmosphere in an ultrasonic bath (99 W, 28 kHz) at room temperature for 15 min. Five milliliters of FLU- $C_nH_{2n+1}SO_3/LDH$ suspension was dropped onto a Si wafer and dried in a vacuum at ambient temperature for 5 h.

2.4. Techniques of Characterization. The powder XRD measurements were performed on a Rigaku XRD-6000 diffractometer, using Cu K α radiation ($\lambda = 0.15418$ nm) at 40 kV, 30 mA, with a scanning rate of 5°/min, and a 2θ angle ranging from 3° to 65°. SEM images were obtained using a Hitachi S-4700 scanning electron microscope operating at 20 kV. The UV-vis spectra were collected in a Shimadzu U-3000 spectrophotometer. Elemental analysis samples were prepared by dissolving 30 mg of solid sample with a few drops of concentrated HNO_3 and diluted to 50 mL with water. Zn and Al elemental analysis was performed by atomic emission spectroscopy with a Shimadzu ICPS-7500 instrument. C, H, and N content was determined using an Elementar vario elemental analysis instrument. The water content of the sample was obtained by thermogravimetry. The FLU content was determined by quantitative analysis of fluorescence with RF-5301PC fluorophotometer. Fluorescence was observed using a OLYMPUS-BX51 fluorescence microscope. The photobleaching was tested by the UV light with CHF-XQ 500W.

Steady-state and time decay polarized photoluminescence measurements were recorded with an Edinburgh Instruments' FLS 920 fluorometer. This instrument is equipped with an emission double monochromator and has a time resolution of 30 ps after deconvolution of the excitation pulse. The emission spectra and lifetime were measured by exciting the samples at 490 nm with a 450 W Xe lamp and nanosecond flashlamp,

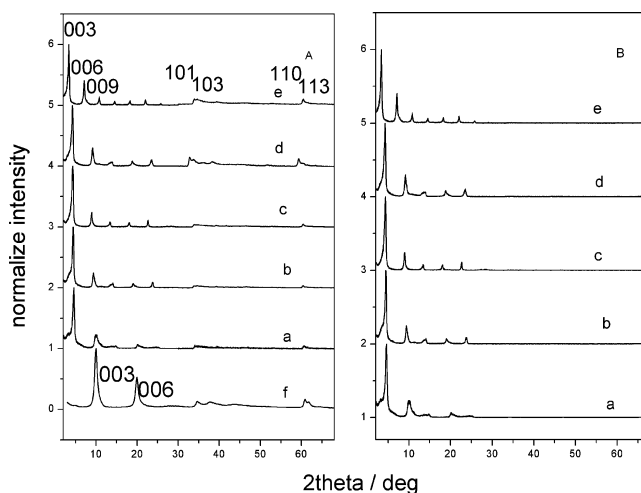


Figure 1. (A) XRD patterns for powder samples (a)–(e) FLU- $C_nH_{2n+1}SO_3/LDH$ and (f) Zn_2Al-NO_3 LDH and (B) XRD patterns for the thin film samples (a)–(e) FLU- $C_nH_{2n+1}SO_3/LDH$ ($n = 5, 6, 7, 10$, and 12, respectively).

respectively. The erratic scattering signal of the laser was eliminated in the detection channel by filtering the excitation light with a 450 nm cutoff filter. The lifetime of the samples was obtained from the recorded decay curves after deconvolution of the instrument response function (IRF) carried out by an iterative method of nonlinear least-squares based on the Marquardt algorithm. The IRF signal was collected on a $C_nH_{2n+1}SO_3/LDH$ film samples without FLU at 490 nm.

Fluorescence polarization emission spectra were recorded on a Quanta Master-Spectrofluorometer (model QM-4/2005). The three-dimensional perspective for the experimental setup was provided in the electronic Supporting Information (Figure S2, Supporting Information). The fluorescence polarization spectra were registered after excitation at 490 nm for the FLU- $C_nH_{2n+1}SO_3/LDH$ thin films, where the fluorescence emission was collected along the Z -axis at 90° with respect to the excitation beam in the Z -axis. The fluorescence polarization spectra were scanned in the range 500–700 nm every 1 nm, with an integration time of 2 s and excitation and emission slits of 4 nm. The orientation of the thin film with respect to the excitation beam was changed by rotating the solid-sample holder around its vertical y -axis. Indeed, the angle between the normal to the thin film and the excitation axis (defined as the δ angle in Figure S2, Supporting Information) was scanned from 0° to 50°. The instrumental response to the linearly polarized light has been corrected by recording the fluorescence signal of an isotropic system under identical experimental conditions. In the present work, the FLU- $C_nH_{2n+1}SO_3/LDH$ powder samples were used as the isotropic system for the thin films of FLU- $C_nH_{2n+1}SO_3/LDH$.

3. Results and Discussion

3.1. Macroscopic Orientation of the FLU- $C_nH_{2n+1}SO_3/LDH$ Thin Films. The XRD patterns of the Zn_2Al-NO_3 LDH and FLU- $C_nH_{2n+1}SO_3/LDH$ are shown in Figure 1. All the patterns of these samples can be indexed to a hexagonal lattice. The interlayer spacing can be calculated from averaging the positions of the three harmonics: $c = 1/3 (d_{003} + 2d_{006} + 3d_{009})$. The (003) reflection of the Zn_2Al-NO_3 LDH powder sample at $2\theta = 9.9^\circ$ (Figure 1A curve f) shows an interlayer distance of 0.88 nm. The basal spacing of FLU- $C_nH_{2n+1}SO_3/LDH$ (Figure 1A curves a–e) increases from 1.88 nm ($n = 5$) to 2.64 nm (n

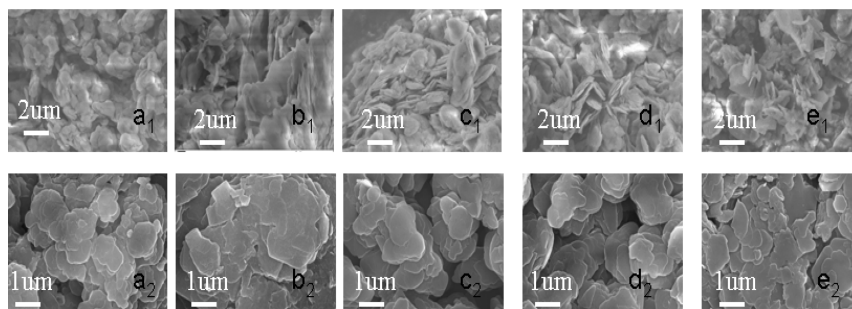


Figure 2. SEM images for the FLU- $C_nH_{2n+1}SO_3$ /LDH powder samples (a₁)–(e₁) and thin film samples (a₂)–(e₂) ($n = 5, 6, 7, 10,$ and 12 , respectively).

= 12), indicating the cointercalation of $C_nH_{2n+1}SO_3$ and FLU in the LDH galleries. The variation of the basal spacing can be attributed to the different arrangements of interlayer guests resulting from the effect of surfactant. It can be seen that the FLU- $C_nH_{2n+1}SO_3$ /LDH thin films (Figure 1B) display only one series of 00 l reflections, indicating a highly ordered stacking of the ab plane of the LDH platelet parallel to the substrate. The half-peak width (fwhm) of (003) reflection (0.33–0.42°) for all the FLU- $C_nH_{2n+1}SO_3$ /LDH samples (Figure S3-B, Supporting Information) is less than that of the precursor Zn_2Al-NO_3-LDH (0.75°) (Figure S3-A, Supporting Information); i.e., no broadening of (003) reflection occurs after cointercalation of FLU and $C_nH_{2n+1}SO_3$. This indicates that FLU and $C_nH_{2n+1}SO_3$ disperse uniformly in the LDH galleries, forming a homogeneous phase. The FT-IR spectra further confirmed the cointercalation of the two anions (Figure S4, Supporting Information) and formation of hydrogen bonding between FLU and surfactant (Figure S5, Supporting Information). Furthermore, FLU and $C_nH_{2n+1}SO_3$ ($n = 5, 12$) cointercalated LDH composites show preferable photoluminescence properties with the molar ratio of FLU/ $C_nH_{2n+1}SO_3$ ($n = 5, 12$) ranging in 10^{-4} – 10^{-3} (Figure S6, Supporting Information), so the sample with FLU/ $C_nH_{2n+1}SO_3 = 10^{-3}$ was chosen for further study in the next section. The chemical compositions of resulting products (Table S1, Supporting Information) show that the experimental ratio of FLU/ $C_nH_{2n+1}SO_3$ in FLU- $C_nH_{2n+1}SO_3$ /LDH composites is close to the nominal ratio, as expected.

SEM images of the FLU- $C_nH_{2n+1}SO_3$ /LDH samples are displayed in Figure 2. The powder samples of FLU- $C_nH_{2n+1}SO_3$ /LDH afford a rough surface and high magnification SEM images (Figure 2a₁–2e₁) reveal that they are composed of randomly oriented LDH particles with irregular morphology. In contrast, the surface of the FLU- $C_nH_{2n+1}SO_3$ /LDH thin films is relatively smooth in the high magnification (Figure 2a₂–2e₂), indicating that the individual FLU- $C_nH_{2n+1}SO_3$ /LDH platelets are densely packed on the substrate plane. The SEM images confirm that the thin films are fabricated with well c -orientation of FLU- $C_nH_{2n+1}SO_3$ /LDH platelets (ab plane parallel to the substrate), consistent with their XRD results in Figure 1.

3.2. Photoluminescence Properties of the FLU- $C_nH_{2n+1}SO_3$ /LDH Thin Films. **3.2.1. UV-Vis Absorption and Fluorescence Emission Spectra of FLU in Solution and the FLU- $C_nH_{2n+1}SO_3$ /LDH Thin Films.** The UV-vis absorption and fluorescence emission spectra of FLU in solution and the FLU- $C_nH_{2n+1}SO_3$ /LDH films were measured and displayed in Figure 3. The UV-vis absorption band of FLU- $C_nH_{2n+1}SO_3$ /LDH (Figure 3A curve a–e) becomes broader than that of the FLU solution sample (Figure 3A curve f), as a result of homogeneous broadening due to the existence of a continuous set of vibrational sublevels in each electronic state.¹² In addition, an obvious red shift was observed for the spectra of FLU- $C_nH_{2n+1}SO_3$ /LDH samples compared with the spectra of the FLU solution,

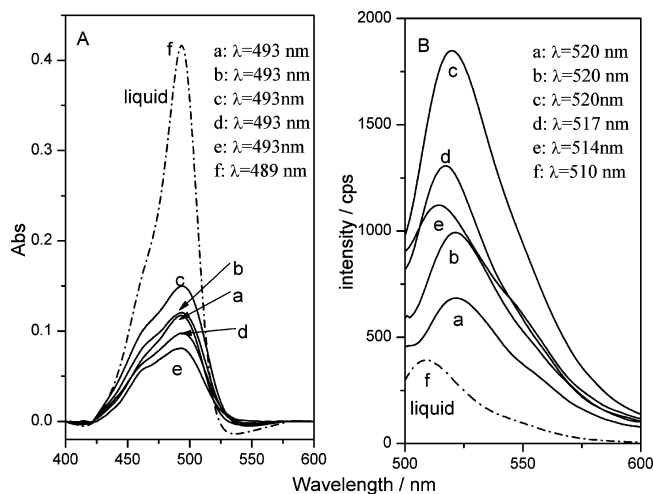


Figure 3. (A) UV-vis absorption spectra of the FLU- $C_nH_{2n+1}SO_3$ /LDH thin film samples for (a)–(e) ($n = 5, 6, 7, 10,$ and 12 , respectively) and (f) pristine FLU in solution. (B) The photoemission spectra of FLU- $C_nH_{2n+1}SO_3$ /LDH thin film samples for (a)–(e) ($n = 5, 6, 7, 10,$ and 12 , respectively) and (f) pristine FLU in solution with the excitation wavelength of 490 nm.

demonstrating that the LDH matrix provides a more rigid and constrained environment for FLU, resulting in a more ordered and dense packing of FLU molecules and an intramolecular charge-transfer character to the π – π transition.¹³ With increasing n value (from 5 to 12 in Figure 3A), the maximum absorption band of the FLU- $C_nH_{2n+1}SO_3$ /LDH thin films shows no shift, indicating that the state of interlayer FLU molecule remains unchanged. In addition, a blue shift of fluorescence emission wavelength from 520 to 514 nm was observed as n increases from 5 to 12 (Figure 3B), due to the change in microenvironment of interlayer FLU molecule.

The fluorescence quantum yield was calculated by the ratio between fluorescence intensity (determined from the integral of the peak) and absorbance at the excitation wavelength (I_{fl}/A_{exc}),¹⁴ as shown in Figure 4. The corresponding fluorescence microscopic photographs are illustrated in Figure S7 (Supporting Information). Both the fluorescence quantum yield and brightness increase at first to a maximum and then decrease as the surfactant length increases (Figure 4 and Figure S7, Supporting Information, respectively). The optimal fluorescence quantum yield presents in the sample with $n = 7$ and the emission peak appears at 520 nm with the fwhm of ca. 30 nm owing to the S_1 – S_0 transition, parallel to the long axis of FLU.¹⁵ This indicates that the cointercalation of $C_nH_{2n+1}SO_3$ surfactant is effective for inhibiting the aggregation of interlayer FLU, which can be explained by the “size-matching” rule between the FLU molecule (1.10 nm, Figure S1, Supporting Information, calculated by Gaussian 03) and the $C_nH_{2n+1}SO_3$ surfactant with $n = 7$ (1.12 nm, Figure S1, Supporting Information). In the case of

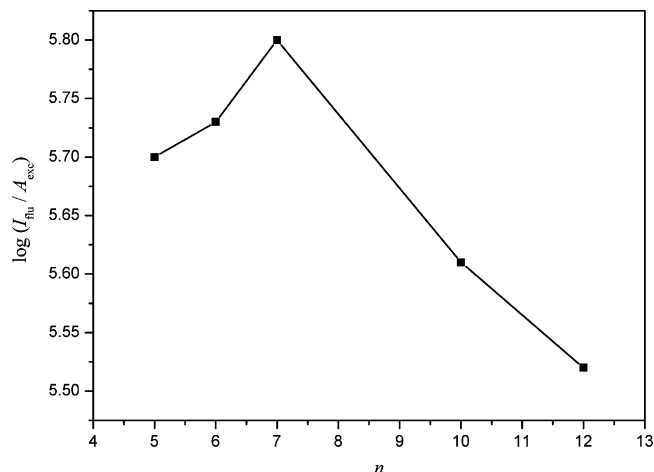


Figure 4. Fluorescence quantum yield varying with the increase of n for the FLU- $C_nH_{2n+1}SO_3/LDH$ samples ($n = 5, 6, 7, 10,$ and 12 , respectively).

TABLE 1: Fluorescence Decay Data of FLU in Solution and the FLU- $C_nH_{2n+1}SO_3/LDH$ Thin Film Samples^a

n	x	τ_i (ns)	A_i (%)	$\langle \tau \rangle$ (ns)	χ^2
5	2	0.93	53.4	2.44	1.12
		4.18	46.6		
6	2	0.88	53.6	2.51	1.45
		4.41	46.4		
7	2	1.05	55.2	2.56	1.24
		4.42	44.8		
10	2	1.36	63.8	2.46	1.35
		4.40	36.2		
12	2	1.10	60.3	2.41	1.41
		4.40	39.7		
solution/ 10^{-5} mol/L	1	1.80	100	1.80	1.22

^a x is the series of exponential fit; τ_i is the fluorescence lifetime; A_i is the preexponential factor related with the statistical weights of each exponential; $\langle \tau \rangle$ is the intensity average lifetime. The goodness of fit is indicated by the value of χ^2 .

$n \neq 7$, the size-mismatching may lead to the formation of FLU aggregates, consequently resulting in the decrease of fluorescence quantum yield. Therefore, the results indicate that the fluorescence properties of interlayer chromophore can be tuned by varying the alkyl chain length of the coexisting surfactant, for the purpose of developing new solid luminescence materials.

3.2.2. Fluorescence Lifetime of FLU in Solution and the FLU- $C_nH_{2n+1}SO_3/LDH$ Thin Films. To further understand the influence of surfactant length on the photoluminescence properties of dye, FLU solution and FLU- $C_nH_{2n+1}SO_3/LDH$ thin film samples were studied by detecting their fluorescence decays, with excitation and emission wavelengths of 490 and 510 nm, respectively. The fluorescence lifetimes were obtained by fitting the decay profiles with a double-exponential form, and the results are listed in Table 1. The multiexponential decay curves were usually observed in solid samples, which can be attributed to the highly heterogeneous environments for chromophores in the solid surfaces.¹⁵ A similar conclusion has been reported by other researchers in the study of intercalation of Rhodamine 6G (R6G) into Laponite clay.¹⁶ Indeed, several host-guest and guest-guest interactions occur in this system: electrostatic interaction, hydrogen bonding among FLU, LDH, $C_nH_{2n+1}SO_3$, and interlayer water. Owing to the difficulty in providing an appropriate interpretation for the multiexponential decay curves, an average lifetime was used in this work. Figure S8 (Supporting Information) displays the fluorescence lifetime of FLU- $C_nH_{2n+1}SO_3/LDH$ as a function of n . The results show that the

fluorescence lifetime of FLU- $C_nH_{2n+1}SO_3/LDH$ increases significantly as n increases from 5 to 7, while it decreases with further increase of n . As a result, the longest fluorescence lifetime obtained by double-exponential fitting is presented for the sample of FLU- $C_nH_{2n+1}SO_3/LDH$ ($n = 7$), due to the “size-matching” rule between FLU and surfactant mentioned above.

Furthermore, it was found from Figure S8 (Supporting Information) that the fluorescence lifetime of FLU- $C_nH_{2n+1}SO_3/LDH$ is much longer than that of FLU solution (1.80 ns). This possibly originates from the decrease in internal mobility, flexibility, and internal conversion processes of FLU owing to the host-guest interactions between the LDH matrix and FLU. Meanwhile, the introduction of surfactant in the LDH galleries effectively isolates FLU anions. Ogawa and Kuroda¹⁷ reported that surfactants or organic solvents can alter the aggregation of photoactive species. In this work, the intercalated surfactant achieves a nonpolar interlayer microenvironment, which homogeneously dilutes and effectively isolates FLU anions.

3.2.3. Orientation for FLU in the LDH Matrix by the Polarized Fluorescence Technique. In this work, the orientation for FLU in the LDH matrix was investigated by fluorescence polarization method. The responses of the fluorescence spectrum of the dye to the horizontally (H) polarized incident light were recorded by varying the orientation angle δ between the normal to the film and the incident light. A linear relationship between the fluorescence dichroic ratio (D_{HV} defined as the ratio of H and V polarized emission spectra, $D_{HV} \equiv I_{HH}/I_{HV}$) and twist angle δ was established by means of (a right-angle configuration between the excitation and the emission beam):¹⁸

$$(D_{HV})^{\text{cor}} = \frac{I_{HH}}{I_{HV}} \times G = 2\cot^2 \psi + (1 - 2\cot^2 \psi) \cos^2(90 + \delta) \quad (1)$$

where G is the instrumental G factor determined by the recorded fluorescence anisotropy of an isotropic system ($G \equiv (I_{HV}/I_{HH})^{\text{iso}}$). In this work, the FLU- $C_nH_{2n+1}SO_3/LDH$ powder samples were used as the isotropic system (see Experimental Section for further details). From the corresponding slope and/or intercept, the relative orientation of the interlayer FLU can be evaluated by the ψ angle (defined as the angle between the transition moment of FLU and the normal to the LDH host layer).

Figure 5A–E displays the fluorescence spectra of the FLU- $C_nH_{2n+1}SO_3/LDH$ thin films recorded with the emission polarizer in the H (I_{HH}) and V (I_{HV}) directions for different twist δ angles. These fluorescence spectra were corrected for the instrumental response to the emission H and V polarizer, taking into account the evolution of the fluorescence band of an isotropic system with the twist angle δ recorded under identical conditions. The fluorescence intensity for the emission H polarizer decreases by decreasing the twist angle δ from 50° up to 0° (Figure 5A₁–E₁). These evolutions were also observed for the V polarized emission light (Figure 5A₂–E₂). These evolutions corroborate the fluorescence anisotropy behavior of thin films, which is assigned to the preferential orientation of the FLU molecule in LDH galleries.

The evolution of the fluorescence dichroic ratio with the emission wavelength of the FLU- $C_nH_{2n+1}SO_3/LDH$ thin films for different twist δ angles is shown in Figure S9A–E (Supporting Information). For a given δ angle, the $(D_{HV})^{\text{cor}}$ value is practically independent of the emission wavelength, confirming the presence of only one type of FLU species for each sample. For a given emission wavelength, the dichroic ratio of

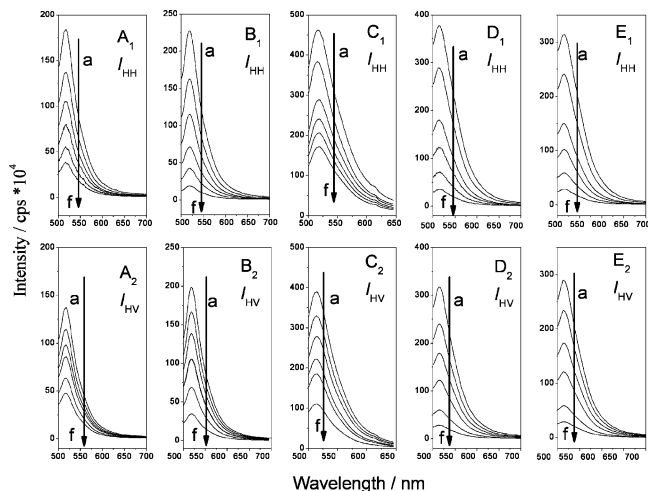


Figure 5. Evolution of the H (A₁–E₁) and V (A₂–E₂) polarized fluorescence spectra of the FLU-C_nH_{2n+1}SO₃/LDH thin film samples with $n = 5, 6, 7, 10,$ and 12 , respectively, with the following twist angle δ : (a) 50° , (b) 40° , (c) 30° , (d) 20° , (e) 10° , and (f) 0° . Spectra were recorded after excitation with horizontal polarized light.

the FLU-C_nH_{2n+1}SO₃/LDH thin films linearly correlates with the $\cos^2(90 + \delta)$ value with a good correlation coefficient $r > 0.99$, as shown in the inset of Figure S9 (Supporting Information) at 520 nm. From the slope and intercept of the (D_{HV})^{cor} vs $\cos^2(90 + \delta)$ linear relationship, the orientation Ψ angles of FLU molecule were calculated to be 63° ($n = 5$), 65° ($n = 6$), 67° ($n = 7$), 69° ($n = 10$), and 72° ($n = 12$) (the schematic models are shown in Figure S10, Supporting Information). It was found that the orientation angle of FLU (Ψ) increases from 63° to 72° (the FLU molecule becomes more parallel with respect to the LDH layer) as n increases from 5 to 12, owing to the increase in nonpolarity in the LDH gallery. The shorter chain of surfactant ($n = 5, 6$) cannot effectively prevent the aggregation of FLU molecules, while a longer chain ($n = 10, 12$) possesses strong flexibility that reduces the confinement effect imposed

by the LDH matrix. Both of them lead to the decrease in the fluorescence intensity and lifetime, as discussed in sections 3.2.1 and 3.2.2.

3.2.4. Steady-State Fluorescence Polarization of the FLU-C_nH_{2n+1}SO₃/LDH Thin Films. One of the most common methods to evaluate fluorescence polarization is the measurement of anisotropic value r , which was fully described by Valeur.¹⁹ r can be expressed by the following formula:

$$r = \frac{I_{\parallel} - I_{\perp}}{I_{\parallel} + 2I_{\perp}} \quad \text{or} \quad r = \frac{I_{\text{VV}} - GI_{\text{VH}}}{I_{\text{VV}} + 2GI_{\text{VH}}} \quad (2)$$

where I_{\parallel} and I_{\perp} are the photoluminescence intensity measured in the planes parallel and perpendicular to the excitation radiation, respectively ($G \equiv I_{\text{HV}}/I_{\text{HH}}$); I_{VH} is the photoluminescence intensity obtained with vertical excitation polarized and horizontal detection polarization; and I_{VV} , I_{HV} , and I_{HH} are defined in a similar way. Theoretically, the value of r is in the range from -0.2 (absorption and emission transition dipoles perpendicular) to 0.4 (two transition dipoles parallel, and deviation from this value means a reorientation of the emission dipole moment).

The polarized photoemission spectra of the FLU-C_nH_{2n+1}SO₃/LDH thin films are displayed in Figure 6. It was found that the anisotropic value increases from $r = 0.20$ ($n = 5$) to a maximum $r = 0.26$ ($n = 7$) and then decreases to $r = 0.11$ ($n = 12$) (Figure 6F). The maximum anisotropic value presents in the sample with $n = 7$, further confirming the “size-matching” effect of surfactant on the high orientation of interlayer FLU. Moreover, rather low anisotropic values were observed for the samples with $n = 10$ and 12 , which can be attributed to the high mobility of FLU (including rotation and translation) in the more flexible microenvironment provided by the long-chain surfactant. Therefore, the results above confirm that both the orientation angle (maximal statistical probability) and the anisotropic value (statistical average) of FLU in the LDH matrix can be tuned by varying the alkyl chain length of surfactant.

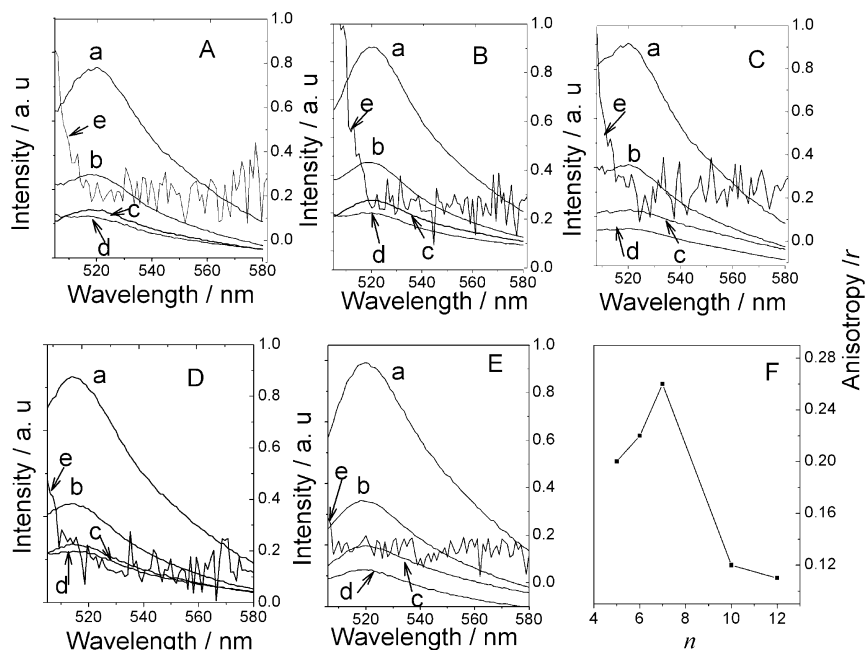


Figure 6. Photoemission profiles in the (a) HH, (b) HV, (c) VH, (d) VV, and (e) polarization and anisotropy of the FLU-C_nH_{2n+1}SO₃/LDH thin film samples for (A) $n = 5$, (B) $n = 6$, (C) $n = 7$, (D) $n = 10$, and (E) $n = 12$, respectively. The excitation wavelength is 490 nm. (F) shows the value of r varying with the increase of n .

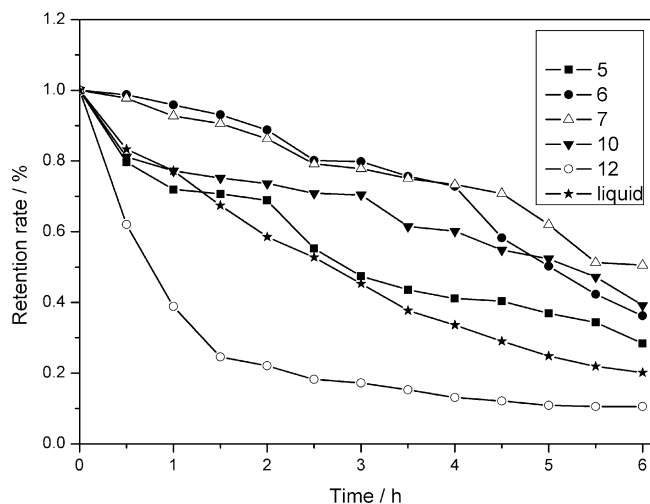


Figure 7. Photostability of the FLU- $C_nH_{2n+1}SO_3/LDH$ thin film samples ($n = 5, 6, 7, 10,$ and 12) and FLU solution as a function of irradiation time. Indicated values are means of three experiments with standard error less than 3%.

3.2.5. Photostability of the FLU- $C_nH_{2n+1}SO_3/LDH$ Thin Films.

The photostability of a dye is of major importance, since it leads to irreversible loss of fluorescence, which limits the statistical accuracy of the detection in biological, environmental, and physiological applications.²⁰ To study the photostability, the fluorescence intensity of the FLU solution and the FLU- $C_nH_{2n+1}SO_3/LDH$ thin films was recorded by illuminating with UV light. Figure 7 displays the fluorescence intensity of the samples as a function of bleaching time. The half-life of the FLU- $C_nH_{2n+1}SO_3/LDH$ thin films with $n \leq 10$ is higher than the FLU solution, while the half-life with $n = 12$ is lower than the FLU solution due to softening the protection from the rigid environment.²¹ The longest half-life presents in the sample of FLU- $C_nH_{2n+1}SO_3/LDH$ ($n = 7, 6$ h), which increases by 2.4-fold compared with that of the FLU solution. The enhancement of photostability demonstrates that the FLU molecule was protected by both the LDH matrix and the coexisting surfactant. First, the LDH offers a confined and stable microenvironment for FLU molecules, enhancing the photostability. van Oijen et al. have reported a similar conclusion in the study of photobleaching of Rhodamine 6G in poly(vinyl alcohol).²² Second, the surfactant molecules uniformly distribute FLU in the LDH matrix and thus reduce the fluorescence quenching effectively. Moreover, the higher anisotropy ($n = 7, r = 0.26$) due to highly ordered orientation of FLU in the LDH gallery enhances the photostability. Therefore, the synergistic effect of the LDH matrix and surfactant plays an important role in obtaining luminous materials with excellent photostability.

4. Conclusion

FLU and $C_nH_{2n+1}SO_3$ were cointercalated between sheets of Zn_2Al LDH by the anion exchange method, and thin films of FLU- $C_nH_{2n+1}SO_3/LDH$ ($n = 5, 6, 7, 10,$ and 12 , respectively) with a well c -orientation verified by XRD and SEM, were obtained by the solvent evaporation method on Si substrates. It was found that the orientation of FLU and its anisotropic value, fluorescence wavelength, emission intensity, and lifetime correlate with the microenvironment of the LDH gallery and can be controlled by changing the alkyl chain length of the surfactant. The optimal fluorescence quantum yield, anisotropy, longest fluorescence lifetime, and

photostability of FLU- $C_nH_{2n+1}SO_3/LDH$ can be obtained with $n = 7$, due to the “size-matching” rule between the organic dye and surfactant. Therefore, this work provides a successful paradigm for accurately modulating photoluminescence properties of chromophore-LDH materials by changing the interlayer microenvironment. The controllability of the aggregate state of the fluorophore as well as its photoluminescence properties (orientation, anisotropy, wavelength, fluorescence quantum yield, and lifetime) based upon the synergistic effect of the LDH matrix and surfactant creates new opportunities for the preparation and application of these intercalation compounds in the fields of photoluminescence materials, nonlinear optics, and polarized luminescence materials.

Acknowledgment. This project was supported by the National Natural Science Foundation of China, the 111 Project (Grant No. B07004), the 973 Program (Grant No. 2009CB939802), and the Fundamental Research Funds for the Central Universities (Grant No. ZZ0908).

Supporting Information Available: Molecular anion structure (Figure S1), three-dimensional perspective for the fluorescence polarized experimental setup (Figure S2), the fwhm of XRD patterns (Figure S3), FT-IR spectra (Figures S4 and S5), the photoemission spectra (Figure S6), fluorescence microscope photographs (Figure S7), fluorescence lifetime as a function of n (Figure S8), evolution of the fluorescence dichroic ratio (Figure S9), and a schematic representation for the orientation of FLU (Figure S10). Chemical compositions (Table S1). This material is available free of charge via the Internet at <http://pubs.acs.org>.

References and Notes

- (1) (a) Zhu, X. L.; Lo, D. *Appl. Phys. Lett.* **2002**, *80*, 917. (b) Nonell, S.; Marti, C.; Garcia-Moreno, I.; Costela, A.; Satre, R. *Appl. Phys. B: Laser Opt.* **2001**, *72*, 355. (c) Yap, S. S.; Tou, T. Y.; Ng, S. W. *Jpn. J. Appl. Phys.* **2000**, *39*, 5855 (Part 1). (d) Yang, Y.; Wang, G. D.; Qian, Z. Y.; Wang, Y.; Hong, Z.; Fan, X. P.; Chen, J. *Mater. Lett.* **2002**, *57*, 660. (e) Schulz-Ekloff, G.; Wohrle, D.; van Duffel, B.; Schoonheydt, R. A. *Microporous Mesoporous Mater.* **2002**, *51*, 91.
- (2) (a) Saito, T.; Kadokawa, J. I.; Tagaya, H. *Trans. Mater. Res. Soc. Jpn.* **2001**, *26*, 503. (b) Hwang, S. H.; Han, Y. S.; Choy, J. H. *Bull. Korean Chem. Soc.* **2001**, *22*, 1019. (c) Williams, G. R.; Fogg, A. M.; Sloan, J.; Tavio-Guého, C.; O'Hare, D. *J. Chem. Soc., Dalton Trans.* **2007**, 3499. (d) Williams, G. R.; O'Hare, D. *J. Mater. Chem.* **2006**, *16*, 3065.
- (3) Costantino, U.; Coletti, N.; Nocchetti, M.; Aloisi, G. G.; Elisei, F.; Latterini, L. *Langmuir* **2000**, *16*, 10351.
- (4) Yan, D. P.; Lu, J.; Wei, M.; Evans, D. G.; Duan, X. *J. Phys. Chem. B* **2009**, *113*, 1381.
- (5) (a) Bauer, J.; Behrens, P.; Speckbacher, M.; Langhals, H. *Adv. Funct. Mater.* **2003**, *13*, 241. (b) Gago, S.; Costa, T.; de Melo, J. S.; Gonçalves, I. S.; Pillinger, M. *J. Mater. Chem.* **2008**, *18*, 894.
- (6) (a) Sasai, R.; Iyi, N.; Fujita, T.; Takagi, K.; Itoh, H. *Chem. Lett.* **2003**, 32, 550. (b) Bujdák, J.; Iyi, N. *Chem. Mater.* **2006**, *18*, 2618.
- (7) (a) Arbeloa, L.; Ojeda, P. R.; Arbeloa, I. L. *Chem. Phys. Lett.* **1988**, *148*, 253. (b) Arbeloa, F. L.; Ojeda, P. R.; Arbeloa, I. L. *J. Chem. Soc. Faraday Trans.* **1988**, *284*, 1903. (c) Aguirresacona, I. U.; Arbeloa, F. L.; Arbeloa, I. L. *J. Chem. Educ.* **1989**, *66*, 866. (d) Arbeloa, F. L.; Aguirresacona, I. U.; Arbeloa, I. L. *Chem. Phys.* **1989**, *130*, 371. (e) Bujdák, J.; Iyi, N. *Chem. Mater.* **2006**, *18*, 2618.
- (8) Shi, W. Y.; Wei, M.; Lu, J.; Evans, D. G.; Duan, X. *J. Phys. Chem. C* **2009**, *113*, 12888.
- (9) (a) Bissell, R. A.; de Silva, A. P.; Gunarathe, H. Q. N.; Lynch, P. L. M.; McCoy, C. P.; Maguire, G. E. M.; Sandanayake, K. R. A. S. In *Fluorescent Chemosensors for Ion and Molecule Recognition*; Czarnik, A. W., Ed.; ACS Symposium Series 538; American Chemical Society: Washington, D.C., 1993; Chapter 9. (b) Walkup, G. K.; Burdette, S. C.; Lippard, S. J.; Tsien, R. Y. *J. Am. Chem. Soc.* **2000**, *122*, 5644. (c) Hirano, T.; Kikuchi, K.; Urano, Y.; Higuchi, T.; Nagano, T. *J. Am. Chem. Soc.* **2000**, *122*, 12399. (d) Setsukinai, S.; Urano, Y.; Kakinuma, K.; Majima,

H. J.; Nagano, T. *J. Biol. Chem.* **2003**, *278*, 3170. (e) Wang, Y. P.; Han, P.; Xu, H.; Wang, Z. Q.; Zhang, X.; Kabanov, A. V. *Langmuir* **2010**, *26*, 709.

(10) (a) Neckers, D. C.; Valdes, A. O. M. In *Advances in Photochemistry*; Volman, D., Hammond, G. S., Neckers, D. C., Eds.; John Wiley & Sons: New York NY, U.S., 1993; Vol. 18. (b) Owen, C. S. *Anal. Biochem.* **1992**, *204*, 65. (c) Tung, C. H. *Biopolymers* **2004**, *76*, 391. (d) Taquet, J. P.; Frochot, C.; Manneville, V.; Barberi, H. M. *Curr. Med. Chem.* **2007**, *14*, 1673. (e) Oh, J. M.; Choi, S. J.; Lee, G. E.; Han, S. H.; Choy, J. H. *Adv. Funct. Mater.* **2009**, *19*, 1617. (f) Xu, Z. P.; Niebert, M.; Porazik, K.; Walker, T. L.; Cooper, H. M.; Middelberg, A. P. J.; Gray, P. P.; Bartlett, P. F.; Lu, G. Q. *J. Controlled Release* **2008**, *130*, 86.

(11) Bontchev, P. P.; Liu, S.; Krumhansl, J. L.; Voigt, J. *Chem. Mater.* **2003**, *15*, 3669.

(12) Nemkovich, N. A.; Rubinov, A. N.; Tomin, I. T. *Inhomogeneous Broadening of Electronic Spectra of Dye Molecules in Solutions*; Lakowicz, J. R. *Topics in Fluorescence Spectroscopy*; Springer: New York, NY, U.S., 1991; Vol. 2, p 367.

(13) Valeur, B. *Molecular Fluorescence: Principles and Applications*; Wiley-VCH: Weinheim, Germany, 2002; p 58.

(14) Martínez, V. M.; Arbeloa, F. L.; Prieto, J. B.; López, T. A.; Arbeloa, I. L. *Langmuir* **2004**, *20*, 5709.

(15) (a) del Monte, F.; Levy, D. *J. Phys. Chem. B* **1998**, *102*, 8041. (b) Latterini, L.; Nocchetti, M.; Aloisi, G. G.; Costantino, U.; Schryver, F. C. D.; Elisei, F. *Langmuir* **2007**, *23*, 12337.

(16) (a) Rurack, K.; Hoffman, K.; Al-Soufi, W.; Resch, G. U. *J. Phys. Chem. B* **2002**, *106*, 9744. (b) Wiederrecht, G. P.; Sandi, G.; Carrado, K. A.; Seifert, S. *Chem. Mater.* **2001**, *13*, 4233.

(17) (a) Michl, J.; Thulstrup, E. W. *Spectroscopy with Polarized Light*; VCH Publishers: New York, NY, U.S., 1986. (b) Kliger, D. S.; Lewis, J. W.; Randall, C. E. *Polarized Light in Optics and Spectroscopy*; Academic Press, Inc.: London England, 1990.

(18) (a) López, A. F.; Martínez, M. V. *J. Photochem. Photobiol. A: Chem.* **2006**, *181*, 44.

(19) Valeur, B. *Molecular Fluorescence: Principles and Applications*; Wiley-VCH, Verlag: Berlin, Germany, 2001; p 131.

(20) Dalvi-Malhotra, J.; Chen, L. H. *J. Phys. Chem. B* **2005**, *109*, 3873.

(21) (a) Hou, Y. W.; Higgins, D. A. *J. Phys. Chem. B* **2002**, *106*, 10306. (b) Hou, Y. W.; Bardo, A. M.; Martinez, C.; Higgins, D. A. *J. Phys. Chem. B* **2000**, *104*, 212.

(22) (a) van Oijen, A. M.; Ketelaars, M.; Köhler, J.; Aartsma, T. J.; Schmidt, J. *Science* **1999**, *285*, 400. (b) Mei, E.; Tang, J. Y.; Vanderkooi, J. M.; Hochstrasser, R. M. *J. Am. Chem. Soc.* **2003**, *125*, 2730. (c) Zondervan, R.; Kulzer, F.; Kol'chenko, M. A.; Orrit, M. *J. Phys. Chem. A* **2004**, *108*, 1657.

JP1069863